solved for the case in which $\epsilon$ follows a normal distribution. The results are given below:

| | Probability of Failure (%) | |
|---|---|---|
| Loading Condition | Uniform $\epsilon$ | Normal $\epsilon$ |
| Static | 7.4 | 7.4 |
| Seismic | | |
| Bayesian | 21.9 | 22.8 |
| Non-Bayesian | 27.7 | 28.5 |

It can be seen that the two distributions of $\epsilon$ give almost identical values for the probability of failure.

## SUMMARY AND CONCLUSIONS

This paper has presented a probabilistic approach to determination of the short-term stability of slopes under static and seismic conditions. Two important uncertainties were considered: (a) the uncertainty in soil strength and its spatial variation and (b) the uncertainty in the method of analysis used. The developed approach was illustrated in an example, and the results obtained were presented and discussed.

On the basis of the analysis and results of this study, the following conclusions are drawn:

1. The probability of failure of slopes can be determined by exploring the uncertainties involved in both material strength and method of analysis.
2. The effect of seismic conditions on the reliability of slopes can be accounted for by using Bayes' theorem.

## ACKNOWLEDGMENT

The work discussed in this paper was part of a research study conducted at Rensselaer Polytechnic Institute and partly supported by the National Science Foundation.

## REFERENCES

1. D.W. Taylor. Fundamentals of Soil Mechanics. Wiley, New York, 1948.
2. K. Terzaghi and R.B. Peck. Soil Mechanics in Engineering Practice. Wiley, New York, 1967.
3. A. Nakase. Stability of Low Embankments on Cohesive Soil Stratum. Journal of Japanese Society of Soil Mechanics and Foundation Engineering, Vol. 10, No. 4, 1970, pp. 40-64.
4. A. Papoulis. Probability, Random Variables, and Stochastic Processes. McGraw-Hill, New York, 1965.
5. J.A. Hooper and F.G. Butler. Some Numerical Results Concerning the Shear Strength of London Clay. Geotechnique, Vol. 16, 1966, pp. 282-304.
6. P. Lumb. The Variability of Natural Soils. Canadian Geotechnical Journal, Vol. 3, May 1966, pp. 74-97.
7. M. Matsuo and A. Asaoka. Probability Models of Undrained Strength of Marine Clay Layer. Journal of Japanese Society of Soil Mechanics and Foundation Engineering, Soils and Foundations, Vol. 17, No. 3, 1977, pp. 1-16.
8. M. Matsuo and A. Asaoka. A Statistical Study on a Conventional Safety Factor Method. Journal of Japanese Society of Soil Mechanics and Foundation Engineering, Soils and Foundations, Vol. 16, No. 1, 1976, pp. 75-90.
9. A.W. Bishop and L. Bjerrum. The Relevance of the Triaxial Test to Solution of Stability Problems. Proc., ASCE Special Conference on Shear Strength of Cohesive Soils, Boulder, CO, 1960, pp. 437-501.
10. D. Athanasiou-Grivas. Probabilistic Evaluation of Safety of Soil Structures. Journal of Geotechnical Engineering Division, ASCE, Vol. 105, No. GT9, Sept. 1979, pp. 1091-1095.
11. D. Athanasiou-Grivas, J. Howland, and P. Tolscer. A Probabilistic Model of a Seismic Slope Stability Analysis. Renssalaer Polytechnic Institute, Troy, NY, Rept. CE-79-1, 1979.

*Publication of this paper sponsored by Committee on Mechanics of Earth Masses and Layered Systems.*

# Model for Assessing Slope Reliability

KEVAN D. SHARP, LOREN R. ANDERSON, DAVID S. BOWLES, AND RONALD V. CANFIELD

**Traditionally, an evaluation of the safety of slopes has been based on computing a safety factor against failure. In computing the safety factor, the geometry of the slope, the soil parameters, and the pore pressures are treated as deterministic quantities even though they are known to be random variables. Vanmarcke has developed a three-dimensional probabilistic slope-stability model that treats shear strength as a random variable. The model uses the probability of a slope failure as an assessment of slope reliability. A probabilistic slope-stability model that is an extension of Vanmarcke's model is presented. The model can accommodate zoned embankments of soil in which the strength is described by the Mohr-Coulomb strength envelope. Autocorrelation functions are used to describe the spatial variation of the mean and standard deviation of the strength parameters, c and tan $\phi$. Several examples are presented to illustrate the influence of the choice of the statistical soil parameters on the probability of failure. The results show that the critical failure surface based on the minimum safety factor is not necessarily the failure surface that will yield the maximum probability of failure.**

The safety of embankments depends on many factors, including the correctness of design assumptions, the adequacy of quality control during construction, the level of inspection and maintenance, the skill of the operators where the embankment impounds water, and the occurrence of various natural phenomena such as floods, earthquakes, and landslides. A complete evaluation of all of the factors that contribute to embankment safety is very complex, and procedures for developing and using this type of information in benefit/cost analyses are still in the formulative stages. The Federal Coordinating Council for Science Engineering and Technology (1) has identified the application of probabilistic methods and risk analysis to dam project development as an important area that needs research. Although progress is be-

ing made on the estimation of overall embankment reliability in relation to a broad range of factors (2,3), much of the progress to date has been made in the area of probabilistic slope-stability analysis. Probabilistic slope-stability analysis is an important consideration and more work is needed, but it should be emphasized that it is only a small part of assessing overall embankment reliability.

Many researchers (4-9) have made contributions to probabilistic slope-stability analysis. Vanmarcke's probabilistic slope-stability model (9) considers the spatial variation of the shear strength along the embankment axis. This paper describes an enhancement of Vanmarcke's (9) model to accommodate effective stress conditions in zoned embankments and also describes a probabilistic slope-stability computer program based on the enhanced model. The model uses the autocorrelation function to evaluate variance reduction rather than the scale of fluctuation recommended by Vanmarcke. The probabilistic technique was incorporated as an option in a slope-stability computer program developed by Bailey (10).

## ANALYSIS OF SLOPE STABILITY

The safety factor for a particular slope and trial failure arc (see Figures 1 and 2) is defined as the ratio of the resisting moment ($M_r$) to the driving moment ($M_o$) about the trial center "O". For a homogeneous embankment of cohesive soil, the safety factor can be stated as

$$F_b = \text{resisting moment/driving moment} = M_{r,b}/M_{o,b} = (s_u Lrb + R_e)/Wab \quad (1)$$

where

$F_b$ = safety factor where subscript b indicates dependence on length of the failure mass,
$s_u$ = design value of undrained shear strength,
L = arc length of failure surface,
r = radius of failure mass,
$R_e$ = contribution of end sections of the failure mass to the resisting moment,
W = weight of the failure mass per unit length,
a = horizontal distance from trial center O to center of gravity of the failure mass, and
b = width of the failure mass.

Figure 1. Typical cylindrical failure mass of an earth embankment.

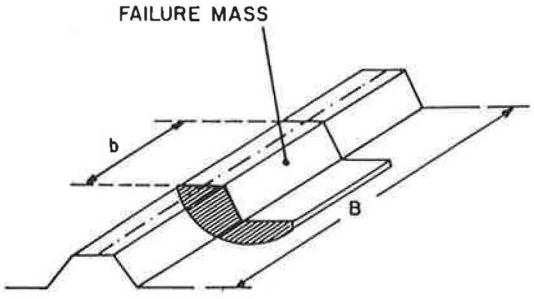


Figure 2. Typical cross section of failure mass.

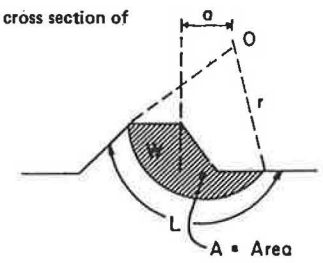


In conventional slope-stability analysis, it is customary to ignore the contribution of $R_e$ to the resisting moment. Thus, Equation 1 becomes

$$F = M_r/M_o = s_u Lr/Wa \quad (2)$$

Although a minimum safety factor is achieved in a conventional slope-stability analysis, the reliability of the slope against a failure in slope stability is unknown. In computing the safety factor from Equation 2, the value of the shear strength ($s_u$) is generally pessimistically selected on the basis of judgment and only limited shear-strength test results.

The design engineer calculates the safety factor for many different trial failure arcs with different center points and radii. The design is then modified so that the minimum safety factor is equal to or larger than the minimum safety factor usually accepted by the profession.

## PROBABILITY OF SLOPE FAILURE

In a probabilistic slope-stability analysis, the critical failure arc is defined as the arc with the largest value of probability ($F < 1.0$) in contrast to the conventional analysis, in which it is defined as the arc with the smallest safety factor. The consideration of shear-strength variability in the probabilistic approach will not necessarily lead to the same design as the conventional slope-stability analysis, which does not explicitly include variability in shear strength.

## DEVELOPMENT OF PROBABILISTIC SLOPE-STABILITY MODEL

In order to evaluate the probability of failure, it is necessary to determine the mean safety factor ($\bar{F}_b$) and the standard deviation of the safety factor ($\tilde{F}_b$).

The mean safety factor for a cylindrical failure mass of width b was given as Equation 1 and can be stated as

$$\bar{F}_b = (\bar{M}_r\, b + R_e)/M_o b \quad (3)$$

where $\bar{M}_r$ is the mean resisting moment per unit width and $M_o$ is the driving moment per unit width.

### Assumptions

In calculating the standard deviation of the safety factor $\tilde{F}_b$, several simplifying assumptions have been made:

1. The variance of the end-area contribution $R_e$ is neglected. Vanmarcke (9) gives a detailed explanation for this assumption and shows that the inclusion of end-area variance has a negligible effect on the probability of failure.
2. Density and slope geometry are treated as deterministic parameters. Uncertainties in both density and geometry occur in both the driving moment and the resisting moment. Alonso (7) shows that probabilistic consideration of these parameters does not influence the outcome greatly since they occur in the numerator and the denominator of the safety factor equation. By neglecting the uncertainties of density and slope geometry, one can consider the driving moment as a deterministic variable. Since it is also assumed that the embankment cross section is constant along the entire axis of the embankment, variations in the cross section are not treated in this model.

3. Pore-pressure uncertainties are not included in the probabilistic analysis. Errors in evaluating pore pressures arise from several factors, including the inability of the engineer to draw an accurate flow net, the assumptions used in derivation of pore pressure/flow net theory, the computer method used to calculate pore pressures, the variability in permeability in the embankment, and the transient nature of groundwater tables. A worst-case condition is assumed for the analysis as an upper bound. Although pore-pressure uncertainties are realistic, inclusion of the pore-pressure variances at some level below the worst case would merely reduce the probability of failure. In addition, neglecting the pore-pressure variances greatly simplifies the probabilistic solution and incorporates some conservatism in the analysis.

4. A normal distribution of the random variables has been assumed. Lumb (11) and Matsuo (6) present results that justify this assumption.

## Variance of the Safety Factor

Based on the given assumptions, the variance of the factor of safety can be developed. Vanmarcke (9) gives the standard deviation of the safety factor as

$$\tilde{F}_b = \tilde{M}_{r,b}/M_{o,b} \quad (4)$$

where $\tilde{M}_{r,b}$ is the standard deviation of the resisting moment of failure mass of width b and $M_{o,b}$ is the deterministic driving moment of the failure mass of width b.

Since all of the variation in the resisting moment is assumed to be in the shear-strength parameters, the standard deviation of the safety factor can be obtained from Equations 1 and 4 as

$$\tilde{F}_b = \tilde{s}_{ub} Lr/Wa \quad (5)$$

where $\tilde{s}_{ub}$ is the standard deviation of the undrained shear strength averaged over width b and arc length L.

## Variance of Shear Strength

Variations in strength occur naturally in a soil mass; however, the stability of an embankment dam is not affected by very small areas of weakness because these are compensated for by the strength of the adjacent area. Thus, local weaknesses tend to be "averaged out" when the strength of a larger area is considered, even though the point-to-point variation in the shear strength can be quite high. There may be several places in the soil mass where the strength is low or high but only for a short distance. If the average strength over a moving average length b is calculated along the axis of the embankment, the moving average of $s_u$ is much less variable than the point-strength values. As a result, the standard deviation of the average values ($\tilde{s}_{ub}$) is less than the standard deviation of the point values ($\tilde{s}_u$). As the averaging length b is increased, the standard deviation of the averaged shear strength decreases. It is obvious that it is the value of the shear strength averaged over the failure surface and not the local weak or strong values that are important for determining the safety factor. It follows that it is the standard deviation associated with width b and arc length L that is needed in Equation 5 and not the standard deviation of the point-strength values.

The standard deviation of shear strength ($\tilde{s}_{ub}$), averaged over the width of the failure mass b and arc length L, is related to the point standard deviation ($\tilde{s}_u$) by

$$\tilde{s}_{ub} = \Gamma_{s,z}(b)\,\Gamma_{s,\ell}(L)\,\tilde{s}_u \quad (6)$$

where $\Gamma_{s,z}(b)$ is the shear-strength-reduction function along the embankment axis and $\Gamma_{s,\ell}(L)$ is the shear-strength-reduction function along the failure surface. These reduction factors are discussed by Vanmarcke (8) and in the following section of this paper.

## Application to Method of Slices

Equation 4 applies to homogeneous slopes of cohesive soil (the so-called $\phi = 0$ condition). However, many embankments contain more than one material and are constructed from soil for which the strength can be described by the Mohr-Coulomb strength theory. In performing a slope-stability analysis for zoned embankments, it is convenient to use a method of slices such as Bishop's simplified method (12).

Based on the method of slices, the mean safety factor of a failure mass such as that shown in Figures 1 and 2 can be stated as

$$\bar{F}_b = \bar{M}_{r,b}/M_{o,b} = [b\,r\,\Sigma\,(\bar{s}_i\,\Delta\ell_i) + R_e]/b\,\Sigma\,W_i a_i \quad (7)$$

where

$\bar{s}_i$ = mean shear strength of the soil at the base of the ith slice,
$\Delta\ell_i$ = base length of the ith slice,
$W_i$ = weight per unit width of the ith slice, and
$a_i$ = perpendicular distance from the line of action of the $W_i$ to the center of the failure arc.

The mean shear strength at the base of each slice, as shown in Figure 3, can be expressed in terms of the Mohr-Coulomb strength theory as

Figure 3. Slice geometry in method-of-slices analysis.

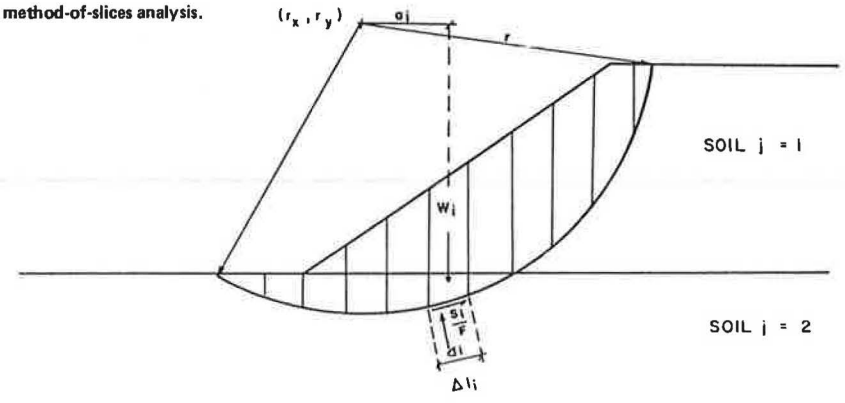

$$\bar{s}_i = \bar{c}_i + \sigma_i \overline{\tan}\ \phi_i \quad (8)$$

where

$\bar{c}_i$ = mean cohesion for the soil at the base of the ith slice,
$\sigma_i$ = normal stress on the failure plane at the base of the ith slice, and
$\overline{\tan}\ \phi_i$ = average coefficient of friction for the soil at the base of the ith slice.

The method of slices can be carried out either as an effective stress analysis or as a total stress analysis. Since pore pressures are treated as deterministic in this model, for simplicity the following development will be in terms of total stress.

For convenience, define an average shear strength for each soil type along the failure plane as

$$\bar{s}_{bj} = [\Sigma(\bar{s}_i \Delta\ell_i)]_j/(\Sigma\Delta\ell_i)_j = [\Sigma(\bar{s}_i\Delta\ell_i)]_j/L_j \quad (9)$$

where $\bar{s}_{bj}$ is the mean shear strength of the jth soil type averaged along the failure plane and $L_j$ is the length of the failure surface passing through the jth soil type.

Equation 7 can now be written as

$$\bar{F}_b = (b\, r\, \Sigma\, \bar{s}_{bj}\, L_j + R_e)/b\, M_o \quad (10)$$

Assuming the strength parameters between soil types to be independent, the standard deviation of the safety factor from Equations 5 and 10 can be expressed as

$$\tilde{F}_b = r\sqrt{\Sigma\, \tilde{s}_{bj}^{\,2}\, L_j^2}/M_o \quad (11)$$

The average shear strength can also be expressed in terms of the Mohr-Coulomb strength theory as

$$\bar{s}_{bj} = \bar{c}_{bj} + (\sigma \overline{\tan}\ \phi)_{bj} \quad (12)$$

where $\bar{c}_{bj}$ is the mean cohesion of the jth soil type averaged along the failure plane and $(\sigma \overline{\tan}\ \phi)_{bj}$ is the mean frictional strength of the jth soil type averaged along the failure plane.

The expression for the standard deviation of shear strength depends on whether or not the cohesion and friction strength components are statistically independent. Matsuo (6) and Lumb (11) have shown that the cohesion and frictional components of shear strength have a slight negative correlation (i.e., there is a slight tendency to have smaller values of cohesion when the friction angle is larger). However, in this paper it is conservatively assumed that the cohesion and friction are independent and that covariance terms can be neglected. Therefore, the standard deviation can be expressed as

$$\tilde{s}_{bj} = [\tilde{c}_{bj}^{\,2} + (\sigma\, \tilde{\tan}\ \phi)_{bj}^{\,2}]^{1/2} \quad (13)$$

Since the shear strength between different soil types is assumed to be uncorrelated, the standard deviation of the safety factor can now be expressed as

$$\tilde{F}_b = \tilde{M}_{r,b}/bM_o = r\left\{\Sigma\, L_j^2\, [\tilde{c}_{bj}^{\,2} + (\sigma\, \tilde{\tan}\ \phi)_{bj}^{\,2}]\right\}^{1/2}/M_o \quad (14)$$

## Probability of Failure

Once the mean and the standard deviation of the safety factor have been found, the probability of failure can be evaluated. The probability of failure of a mass of width b in the embankment is defined as the probability that the safety factor is less than one:

$$P_f(b) = P(F_b < 1) \quad (15)$$

It can be shown that $P_f(b)$ can be calculated based on a standard normal probability density function and the reliability index $\beta_b$, where $\beta_b$ is calculated by

$$\beta_b = (\bar{F}_b - 1)/\tilde{F}_b \quad (16)$$

Unlike conventional slope-stability analysis, the safety factor depends on the width b of the failure mass. Vanmarcke (9) shows that there is a critical width $b_c$ and that it is a function of the end resistance $R_e$, the mean resisting moment $\bar{M}_r$, and the driving moment $M_o$:

$$b_c = R_e/(\bar{M}_r - M_o) \quad (17)$$

This value, $b_c$, should be used to evaluate the mean and standard deviation of the safety factor, $\bar{F}_b$ and $\tilde{F}_b$. It is interesting to note that the critical width, $b_c$, is not a function of the variance properties.

For an embankment with an overall length B that is less than the critical width $b_c$, the probable failure mass includes the entire embankment. However, when the overall embankment width exceeds the critical width, there are many possible placements of the critical width along the embankment; thus, the probability of failure of the embankment increases as the total embankment width increases.

## SPATIAL VARIANCE OF SHEAR STRENGTH

The Mohr-Coulomb theory, as stated in Equation 8, describes the shear strength of soil in terms of cohesion, normal stress, and the tangent of the friction angle.

The point variance of the shear strength is defined as

$$\tilde{s}^2 = E\,(s - \bar{s})^2 \quad (18)$$

where E denotes expected value. In terms of the cohesion and friction components, by using Equation 8 this can be stated as

$$\tilde{s}^2 = E\,(c + \sigma \tan\phi - \bar{c} - \sigma \overline{\tan}\ \phi)^2 \quad (19)$$

or

$$\tilde{s}^2 = \tilde{c}^2 + \sigma^2\, (\tilde{\tan}\ \phi)^2 + 2\sigma\, \mathrm{cov}(c, \tan\phi) \quad (20)$$

where

$\tilde{s}^2$ = point variance of s,
$\tilde{c}^2$ = point variance of c,
$\tilde{\tan}\ \phi^2$ = point variance of tan $\phi$, and
$\mathrm{cov}(c, \tan\phi)$ = covariance of c and tan $\phi$.

As discussed earlier, the covariance in Equation 20 is neglected.

It was explained in a previous section that the standard deviation (square root of the variance) of strength values averaged over some distance is less than the standard deviation of shear strength at a random point. Equation 6 uses reduction functions to relate point standard deviations to the standard deviation averaged over a surface. These reduction functions (in terms of variance) are explained in this section.

The variance of shear strength $\tilde{s}_z^{\,2}$, averaged over a distance Z, can be stated in terms of the point variance as

$$\tilde{s}_z^{\,2} = \Gamma_{s,z}^{\,2}(Z)\, \tilde{s}^2 \quad (21)$$

where $\Gamma_{s,z}^2$ (Z) = shear-strength variance-reduction function for the z direction.

The variance-reduction function describes the decay of variance of a spatial average of a strength parameter as the averaging distance is increased. As the averaging distance approaches zero, the variance of the soil parameter is equal to the point variance.

## Scale of Fluctuation

There are many functional forms that may be used to model the variance-reduction function. Vanmarcke (9,13) describes an approximate form that uses a parameter called the scale of fluctuation ($\delta$), which is a measure of the rate of fluctuation of a soil property about its mean value along a line in the embankment. The variance-reduction function in terms of the scale of fluctuation is

$$\Gamma_{s,z}^2 (Z) = \delta/Z \quad Z > \delta \tag{22}$$

$$\Gamma_{s,z}^2 (Z) = 1 \quad Z \leq \delta \tag{23}$$

## Autocorrelation Functions

Other forms of variance-reduction functions make use of autocorrelation functions, which describe the correlation of strength between two points separated by a given distance. Vanmarcke (9,13) shows a graphical comparison of the various forms of variance-reduction functions. The model developed in this paper uses autocorrelation functions rather than the scale of fluctuation. This method appears to be more versatile when the method of slices is used. Furthermore, the use of autocorrelation functions will allow more flexibility in evaluating field data.

A failure surface of width b and arc length L has a strength variance $\tilde{s}_b^2$, as defined by

$$\tilde{s}_b^2 = E(s_b - \bar{s}_b)^2 \tag{24}$$

where $s_b$ is the average strength at a random location along the embankment over the cylindrical failure surface (Figure 1) and is defined as

$$s_b = (r/Lb) \int_z \int_\theta [c(\Psi, \nu) + \sigma(\Psi) \tan \phi(\Psi, \nu)] \, d\Psi d\nu \tag{25}$$

and $\bar{s}_b$ is the expected value of $s_b$ and is defined as

$$\bar{s}_b = E(s_b) = (r/Lb) \int_z \int_\theta [\bar{c} + \sigma(\Psi) \overline{\tan \phi}] \, d\Psi d\nu \tag{26}$$

Assuming that the variance-reduction functions may be factored into their spatial components, it can be shown that the variance of the strength can be expressed as

$$\begin{aligned} \tilde{s}_b^2 = {} & (r^2 \tilde{c}^2/L^2 b^2) \int_z \int_z \rho_{c,z}(\nu, \nu') d\nu d\nu' \int_\theta \int_\theta \rho_{c,\ell}(\Psi, \Psi') d\Psi d\Psi' \\ & + [r^2 \widetilde{\tan \phi})^2 / L^2 b^2] \int_z \int_z \rho_{\tan \phi, z}(\nu, \nu') d\nu d\nu' \\ & \int_\theta \int_\theta \sigma(\Psi) \sigma(\Psi') \rho_{\tan \phi, \ell}(\Psi, \Psi') d\Psi d\Psi' \end{aligned} \tag{27}$$

where $\rho_{c,z}(\nu,\nu')$, $\rho_{c,\ell}(\Psi,\Psi')$ are autocorrelation functions for cohesion along the axis of the embankment and along the arc length, respectively, and $\rho_{\tan \phi,z}(\nu,\nu')$, $\rho_{\tan \phi,\ell}(\Psi,\Psi')$ are autocorrelation functions for tan $\phi$ along the axis of the embankment and along the arc length, respectively.

Thus, for cohesion, the variance along the arc ($\tilde{c}_\ell^2$) can be described as

$$\tilde{c}_\ell^2 = (r^2 \tilde{c}^2/L^2) \int_\theta \int_\theta \rho_{c,\ell}(\Psi, \Psi') d\Psi d\Psi' \tag{28}$$

Thus, the cohesion variance-reduction function along the arc length becomes

$$\Gamma_{c,\ell}^2 (L) = (r^2/L^2) \int_\theta \int_\theta \rho_{c,\ell}(\Psi, \Psi') d\Psi d\Psi' \tag{29}$$

It can also be shown that the cohesion variance-reduction function along the axis of the embankment can be expressed as

$$\Gamma_{c,z}^2 (b) = (1/b^2) \int_o^b \int_o^b \rho_{c,z}(\nu, \nu') d\nu d\nu' \tag{30}$$

The cohesion variance over the failure surface can now be stated in terms of the cohesion point variance as

$$\tilde{c}_b^2 = \Gamma_{c,z}^2 (b) \, \Gamma_{c,\ell}^2 (L) \, \tilde{c}^2 \tag{31}$$

The variance of tan $\phi$ along the failure arc [$(\widetilde{\tan \phi})_\ell^2$] can be shown to equal

$$(\widetilde{\tan \phi})_\ell^2 = (\widetilde{\tan \phi})^2 (r^2/L^2) \int_\theta \int_\theta \sigma(\Psi) \sigma(\Psi') \rho_{\tan \phi, \ell}(\Psi, \Psi') d\Psi d\Psi' \tag{32}$$

and the friction variance-reduction function along the failure arc becomes

$$\Gamma_{\tan \phi, \ell}^2 (L) = (r^2/L^2) \int_\theta \int_\theta \sigma(\Psi) \sigma(\Psi') \rho_{\tan \phi, \ell}(\Psi, \Psi') d\Psi d\Psi' \tag{33}$$

As in the case of cohesion, the variance of tan $\phi$ over the failure mass can be related to the point variance by

$$(\widetilde{\tan \phi})_b^2 = \Gamma_{\tan \phi, z}^2 (b) \, \Gamma_{\tan \phi, \ell}^2 (L) \, (\widetilde{\tan \phi})^2 \tag{34}$$

where

$$\Gamma_{\tan \phi, z}^2 (b) = (1/b^2) \int_o^b \int_o^b \rho_{\tan \phi, z}(\nu, \nu') d\nu d\nu' \tag{35}$$

A complete derivation of $\tilde{s}_b^2$ is available from the authors on request.

The numerical evaluation of $\Gamma_{s,\ell}^2$(L) along an arc length is not convenient, since spatial variance functions are measured in terms of Cartesian coordinates. Since sampling techniques for the evaluation of variance-reduction functions are not involved with sampling along a given arc, it is necessary to transform variance-reduction functions evaluated in Cartesian coordinates into polar coordinates. The transformation again assumes that autocorrelation functions over a surface area can be factored into their spatial components so that

$$\rho_{s,\ell}(\Psi, \Psi') = \rho_{s,x}(\Delta x) \, \rho_{s,y}(\Delta y) \tag{36}$$

where s is a shear-strength component (either c or tan $\phi$).

The variance functions along an arc can be defined in terms of the autocorrelation functions represented in Cartesian coordinates as

$$\Gamma_{s,\ell}^2 (L) = [1/(\theta_2 - \theta_1)^2] \int_{\theta_1}^{\theta_2} \int_{\theta_1}^{\theta_2} \rho_{s,x}(\Delta x) \, \rho_{s,y}(\Delta y) d\Psi d\Psi' \tag{37}$$

The variance-reduction functions along an arc can be defined in terms of the autocorrelation functions represented in Cartesian coordinates as

$$\rho_{s,x}(\Delta x) = \rho_{s,x}(r|\cos \Psi - \cos \Psi'|) \tag{38}$$

and

$$\rho_{s,y}(\Delta y) = \rho_{s,y}(r|\sin \Psi - \sin \Psi'|) \tag{39}$$

The proper autocorrelation function to be used and its coefficients must be determined from actual field data. A combination of two or more simple, exponentially decaying autocorrelation functions may be necessary to fit the field data curves. Currently, only one form of the autocorrelation function is included in the probabilistic slope-

stability model. These autocorrelation functions in each coordinate direction are

$$\rho_x(\Delta x) = \exp\,[-(\Delta x/k_x)^2] \quad (40a)$$

$$\rho_y(\Delta y) = \exp\,[-(\Delta y/k_y)^2] \quad (40b)$$

$$\rho_z(\Delta z) = \exp\,[-(\Delta z/k_z)^2] \quad (40c)$$

The coefficients $k_x$, $k_y$, and $k_z$ may vary for c and tan $\phi$ for each soil type within an embankment. They control the rate of variance decay with distance.

Variance reduction is performed on $\tilde{c}^2$ and $(\widetilde{\tan}\ \phi)^2$ for each soil type along the failure arc within the embankment. The intersections of each soil boundary with the failure arc are determined in terms of polar coordinates. The intersection coordinates are then used as the limits of integration for the variance-reduction functions. It is not practical to use closed-form solutions to the variance functions, since alternative forms may be necessary. Numerical techniques are used to evaluate $\Gamma_{s,\ell}^2(L)$ and $\Gamma_{s,z}^2(b)$ for both cohesion and tan $\phi$.

## PROBABILISTIC SLOPE-STABILITY COMPUTER MODEL

The theoretical model presented above has been incorporated into a slope-stability-analysis computer program originally developed by Bailey (10). The probabilistic analysis does not begin until the plane-strain safety factor has been computed; therefore, if desired, the program can also be used for conventional deterministic analysis.

There are five main steps in the analysis:

1. Evaluate the plane-strain safety factor $\bar{F}$.
2. Evaluate the resistance of the end areas.
3. Evaluate the critical width $b_c$.
4. Evaluate the variance of resisting moment by computing the three-dimensional variance-reduction functions for cohesion and tan $\phi$.
5. Evaluate the probability of failure.

### Plane-Strain Safety Factor

Bishop's simplified method of slices (12) is used to evaluate the plane-strain safety factor F and to compute the normal stresses along the failure arc. The format of the program is essentially the same as that used in ICES LEASE I (14), and the user-machine communication is interactive.

### End-Area Resistance

A typical cross section of an embankment, a failure arc, and the slices used in the deterministic analysis are shown in Figure 3. End-area moment resistance may be found by integrating the moment resistance on a differential element over the end area. The moment resistance on a differential element is given by

$$dM = r(c + K_o\,\sigma \tan \phi)dxdy \quad (41)$$

where $K_o$ is the coefficient for lateral at-rest earth pressure.

Once the end-area resistance has been computed, the critical width can be computed from Equation 17. The factor of safety of the cylindrical failure mass can then be calculated by using Equation 14.

### Variance of Resisting Moment

The variance-reduction integrals for c and tan $\phi$ described in Equations 28-39 are evaluated for each soil type intersected by the failure surface. Values of the variances of resisting moment, $\tilde{M}_r^2$ and $\tilde{M}_{r,b}^2$, are computed separately by first evaluating $\tilde{s}_\ell^2$ and then $\tilde{s}_b^2$ as previously explained, where

$$\tilde{M}_r^2 = r^2 \Sigma\, \tilde{s}_{i\ell}^2\, L_i^2 \quad (42)$$

and

$$\tilde{M}_{r,b}^2 = r^2 \Sigma\, \tilde{s}_{ib}^2\, L_i^2 \quad (43)$$

Equation 33 shows that the computation of the variance-reduction function for tan $\phi$ along the arc length $\Gamma_{\tan\phi,\ell}^2(L)$ requires knowledge about the stresses normal to the failure surface. The normal stresses evaluated at the base of each slice in Bishop's simplified method are used to evaluate the variance-reduction functions. Thus, once the safety factor has been found, the normal forces may be calculated.

The numerical integration of $\Gamma_{s,\ell}^2(L)$ involves subdividing the arc length into finite segments. The value of the normal stress at each segment is then found by interpolating from the normal forces at the midpoint of each slice.

### Probability of Failure

The standard deviation of the safety factor and the reliability index are computed from Equations 11 and 16, respectively, following the evaluation of the variance of the resisting moment. Vanmarcke (9) shows that the probability of failure of a mass of width b is directly related to the reliability index $\beta_b$. Thus, $\beta_b$ is a measure of the probability of failure. The value of b that minimizes the reliability index does not necessarily maximize the probability of failure because $p_f(b)$ and $\beta_b$ have a nonlinear relation. A curve of $p_f(b)$ versus b generally has a relatively flat peak, and it has been found that the value of b that minimizes the reliability index closely maximizes $p_f(b)$ for all practical considerations.

The value of the probability of failure can be computed from the mean and the standard deviation of the safety factor, and it can be assumed that the safety factor follows the normal probability density function. This can be evaluated from the probability integral p(x) of a standardized normal probability density function:

$$p(x) = (2\pi)^{-1/2} \int_{-\infty}^{\beta_b} \exp(-t^2/2)dt \quad (44)$$

Two infinite series, given by Dwight (15), are used in the computer program to evaluate p(x).

The probability of failure of the entire embankment of length B must consider an infinite combination of overlapping failure masses of width b (Figure 1). A moving average of strength is associated with failure surfaces of width b that have center $z_o$ and end coordinates $z_o \pm b/2$, where $z_o$ is randomly located from b/2 to B - b/2.

The probability of failure of the embankment [$P_F(B)$] can be calculated based on the rate of decay of reliability per unit length and the probability of survival of the embankment (9).

## APPLICATION OF THE COMPUTER MODEL

The use of the computer model requires data input for a conventional deterministic analysis as well as the statistical parameters required for the probabilistic analysis. The data required for the conventional analysis include (a) cross-section geometry; (b) soil parameters, including unit weight, cohesion, and friction angle (for a

probabilistic analysis these parameters must be mean values); (c) pore-pressure data; and (d) specifications for the location of the failure surface. The parameters required for the probabilistic analysis include (a) the standard deviation of the strength parameters $\tilde{c}$ and $\widetilde{\tan}\ \phi$ for each soil type, (b) variance decay parameters for cohesion and tan $\phi$, and (c) the total length of the embankment.

The program is currently limited to circular failure surfaces. We are currently enhancing the probabilistic slope-stability analysis to accommodate other shapes of failure surfaces.

## Illustrative Examples

Several example problems were chosen to demonstrate the effects of the variances, the autocorrelation coefficients, and the location of the failure surface on the probability of failure of an embankment.

### Example 1

The embankment shown in Figure 4 illustrates a base failure in a cohesive soil. The embankment is 9.1 m in height and has a 1.5:1 slope. Mean strength properties are shown in Figure 4 and given below:

| Property | Value |
|---|---|
| $\bar{c}$ (kPa) | |
| Soil 1 | 34.97 |
| Soil 2 | 43.11 |
| tan $\phi$ | |
| Soil 1 | 0.213 |
| Center of rotation point | A |
| Embankment width (m) | 229 |
| End-area resistance $R_e$ (kn•m) | $2.95 \times 10^5$ |
| Radius (m) | 17.98 |
| Critical width $b_c$ (m) | 36.9 |
| $\bar{F}$ | 1.35 |
| $\bar{F}_b$ | 1.71 |

The plane-strain safety factor calculated by Equation 2 is 1.35 for the center of rotation at point A. For a cylindrical failure surface, the critical width calculated from Equation 17 is 36.9 m and the safety factor calculated from Equation 10 is 1.71.

For the failure arc of radius 17.98 m (critical point), as shown in Figure 4, several computer trials were run in which the standard deviations of the strength properties were held constant and the autocorrelation coefficients were varied. The results, given in Table 1, list the standard deviation of the safety factor ($\tilde{F}_b$), the reliability index ($\beta_b$), and the probability of failure. Each set of results is tabulated with the coefficients of variation and the variance decay parameters used. The results indicate that, as the variance decay constants increase, $\tilde{F}_b$ increases, thus increasing the probability of failure. It can be seen that the value of these constants plays an important role in the magnitude of the probability of failure.

The last set of trials in Table 1 demonstrates the effect of the point variances on the probability of failure. The autocorrelation coefficients were held constant while the coefficients of variation ($\tilde{c}/\bar{c}$ and $\widetilde{\tan}\ \phi/\overline{\tan}\ \phi$) were decreased by 10 percent. The probability of failure predictably decreased, as indicated in Table 1.

### Example 2

The embankment of example 1 was also used in example 2. The variance properties were held constant while the radii and the location of the center of rotation were varied along a grid, as shown in Figure 4. Table 2 gives the variance properties for example 2, and Table 3 gives the pertinent data that were used for points A and B. It should be noted that the maximum probability of failure does not coincide with the failure surface with the minimum plane-

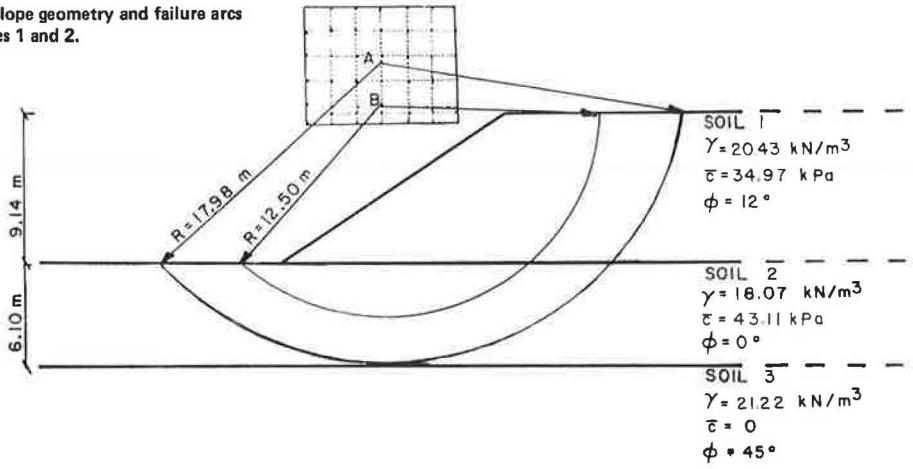


**Figure 4. Slope geometry and failure arcs for examples 1 and 2.**

**Table 1. Results of computer trials for example 1.**

| Trial | $\tilde{c}/\bar{c}$ (%) Soil 1 | $\tilde{c}/\bar{c}$ (%) Soil 2 | $\widetilde{\tan}\ \phi/\tan\ \phi$ (%) Soil 1 | $\widetilde{\tan}\ \phi/\tan\ \phi$ (%) Soil 2 | $k_x, k_z$ (m) Soil 1 | $k_x, k_z$ (m) Soil 2 | $k_y$ (m) Soil 1 | $k_y$ (m) Soil 2 | $\tilde{F}_b$ | $\beta_b$ | $P_F(B)$ |
|---|---|---|---|---|---|---|---|---|---|---|---|
| 1 | 27.4 | 41.7 | 16.4 | 0 | 5.33 | 7.62 | 1.52 | 0.76 | 0.173 | 7.22 | $9.1 \times 10^{-12}$ |
| 2 | 27.4 | 41.7 | 16.4 | 0 | 8.53 | 12.19 | 2.44 | 1.22 | 0.219 | 4.70 | $2.8 \times 10^{-5}$ |
| 3 | 27.4 | 41.7 | 16.4 | 0 | 10.67 | 15.24 | 3.05 | 1.52 | 0.244 | 3.88 | $9.0 \times 10^{-4}$ |
| 4 | 27.4 | 41.7 | 16.4 | 0 | 21.34 | 30.48 | 6.10 | 3.05 | 0.331 | 2.37 | $8.3 \times 10^{-2}$ |
| 5 | 17.4 | 31.7 | 6.4 | 0 | 10.67 | 15.24 | 3.05 | 1.52 | 0.184 | 5.13 | $3.1 \times 10^{-6}$ |
| 6 | 27.4 | 41.7 | 16.4 | 0 | 10.67 | 15.24 | 3.05 | 1.52 | 0.244 | 3.88 | $9.0 \times 10^{-4}$ |

**Table 2. Soil properties for example 2.**

| Soil | $\bar{c}$ (kPa) | $\tilde{c}/\bar{c}$ (%) | $\overline{\tan \phi}$ | $\widetilde{\tan \phi}/\overline{\tan \phi}$ (%) | $k_x, k_z$ (m) | $k_y$ (m) |
|---|---|---|---|---|---|---|
| 1 | 34.97 | 27.4 | 0.213 | 16.4 | 10.67 | 3.05 |
| 2 | 43.11 | 41.7 | 0 | 0 | 15.24 | 1.52 |

Note: Embankment width = 229 m.

**Table 3. Results of computer trials for example 2.**

| Trial | Center of Location | R (m) | $b_c$ (m) | $\bar{F}$ | $\bar{F}_b$ | $\tilde{F}_b$ | $\beta_b$ | $P_F(B)$ |
|---|---|---|---|---|---|---|---|---|
| 1 | A | 17.98 | 36.90 | 1.35 | 1.71 | 0.244 | 3.88 | $9.0\times10^{-4}$ |
| 2 | A | 16.92 | 31.52 | 1.39 | 1.77 | 0.203 | 3.78 | $1.5\times10^{-3}$ |
| 3 | A | 15.70 | 26.35 | 1.42 | 1.85 | 0.231 | 3.66 | $2.7\times10^{-3}$ |
| 4 | A | 14.48 | 20.22 | 1.51 | 2.02 | 0.264 | 3.86 | $1.6\times10^{-3}$ |
| 5 | B | 15.54 | 36.39 | 1.35 | 1.70 | 0.187 | 3.72 | $1.7\times10^{-3}$ |
| 6 | B | 14.02 | 28.40 | 1.40 | 1.80 | 0.221 | 3.63 | $2.8\times10^{-3}$ |
| 7 | B | 12.50 | 22.91 | 1.45 | 1.90 | 0.258 | 3.47 | $5.9\times10^{-3}$ |
| 8 | B | 10.97 | 16.16 | 1.58 | 2.16 | 0.292 | 3.96 | $1.3\times10^{-3}$ |

strain safety factor. This illustrates that the probability of failure depends not only on the plane-strain safety factor but also on the variance decay (dependent on the arc length) and the contribution of the end resistance. A comparison of trials 1 and 7, as given in Table 3, indicates a much higher probability of failure for trial 7 ($5.9\times10^{-3}$) than for trial 1 ($9.0\times10^{-4}$) even though the safety factor for trial 7 is higher than that for trial 1 (1.45 compared with 1.35).

## General Discussion of Results

The values chosen for $\tilde{c}$ and $\widetilde{\tan \phi}$ in the example problems for each soil type are considered to be realistic. Lumb (16) and Matsuo (6) have reported the coefficient of variation for tan $\phi$ [$(\widetilde{\tan \phi}/\overline{\tan \phi})$] to be from 5 to 20 percent and for cohesion [$(\tilde{c}/\bar{c})$] to be from approximately 15 to 40 percent.

There is little information available concerning the typical appropriate values to be used for variance decay parameters. The appropriate values of the probabilistic parameters to be used in the analysis must be determined from rather extensive field studies. The actual form of the autocorrelation function depends on the soil characteristics and its manner of placement. A field study sponsored by the U.S. Bureau of Mines is currently under way. The study involves the variance and correlation properties of mine tailings dams and assessment of their reliability. Preliminary results on a tailings dam have shown the vertical correlation distance, $k_y$, is much smaller than the horizontal correlation distance. Future studies may produce more information regarding the spatial variance properties of particular soil types. Pooling of information from many such studies could assist design engineers in estimating the probabilistic parameters without the need for extreme field studies on any site.

## CONCLUSIONS

A computer model has been developed to perform probabilistic slope-stability analysis. The model is based on an extension of Vanmarcke's probabilistic slope-stability model (9) and can accommodate zoned embankments and soils for which the strength parameters are described by the Mohr-Coulomb strength envelope. The model currently uses a cylindrical failure surface but can easily be extended to other failure-surface shapes by using different formulations for the autocorrelation functions along the failure surface and along the embankment axis. In a statistical sense, the model is three-dimensional because the spatial variation of the strength parameters is considered. The mechanics of the model, however, are two-dimensional except that the resistance at the ends of the cylindrical failure mass is considered. Pore pressures are treated as deterministic parameters and are computed from the location of a piezometric surface from a construction pore-pressure parameter. By determining the probability of failure for various positions of the piezometric surface, a critical pore-pressure condition can be determined. Pore pressures can then be monitored in the field and compared with pore pressures that would produce an unacceptable probability of failure.

A more extensive field and laboratory program will be necessary to define the probabilistic soil parameters than would be required for a conventional analysis. We are currently conducting an extensive field investigation to establish the statistical soil parameters for a tailings dam. As more experience is gained in this area, it should be possible to develop specific guidelines as to the required extent of such an investigation.

Probabilistic analysis appears to be a more rational way to evaluate embankment stability than the conventional safety-factor approach. It has been pointed out that it is possible to have a case in which the probability of failure for one slope is higher than that for a second slope even though the second slope has a lower safety factor. Furthermore, the example problems suggest that the critical failure surface based on the safety factor is not the same as that based on the probability of failure. Probabilistic analysis in itself provides a rational method for evaluating the reliability of slopes, and it will become even more valuable as methods for risk-benefit analysis of earth structures are further developed.

## ACKNOWLEDGMENT

We wish to acknowledge the financial and technical support provided by the Bureau of Mines, U.S. Department of the Interior. We are especially indebted to the technical project officer, Paul C. McWilliams of the Bureau of Mines, for his suggestions and technical advice.

## REFERENCES

1. Improving Federal Dam Safety. Federal Coordinating Council for Science Engineering and Technology, Washington, DC, Nov. 1977.
2. D.S. Bowles, L.R. Anderson, and R.V. Canfield.

A Systems Approach to Risk Analysis for an Earth Dam. International Symposium on Risk and Reliability in Water Resources, Waterloo, Ontario, Canada, 1978.
3. G. Baecher, M. Pate, and R. de Neufville. NED Cost Determination for Probability of Dam Failure. Systems Analysis, Cambridge, MA, Final Rept., May 1979.
4. T. Wu and L.M. Kraft. Safety Analysis of Slopes. Journal of Soil Mechanics and Foundations Division, ASCE, Vol. 96, No. SM2, March 1970, pp. 609-632.
5. D.S. Athanasiou-Grivas. Reliability of Slopes of Particulate Materials. Purdue Univ., West Lafayette, IN, Ph.D. thesis, 1976.
6. M. Matsuo. Reliability in Embankment Design. Department of Civil Engineering, Massachusetts Institute of Technology, Cambridge, Res. Rept. R76-33, July 1976.
7. E.E. Alonso. Risk Analysis of Slopes and Its Application to Slopes in Canadian Sensitive Clays. Geotechnique, Vol. 26, No. 3, 1976, pp. 453-472.
8. E.H. Vanmarcke. Probabilistic Modeling of Soil Profiles. Journal of Geotechnical Engineering Division, ASCE, Vo.. 103, No. GT11, Nov. 1977, pp. 1127-1146.
9. E.H. Vanmarcke. Earth Slope Reliability. Journal of Geotechnical Engineering Division, ASCE, Vol. 103, No. GT11, Nov. 1977, pp. 1247-1268.
10. W.A. Bailey. Stability Analysis by Limiting Equilibrium. Massachusetts Institute of Technology, Cambridge, M.S.C. E. thesis, 1966.
11. P. Lumb. Application of Statistics in Soil Mechanics. In Soil Mechanics--New Horizons, Butterworth and Co., London, England, 1974, pp. 44-111.
12. A.W. Bishop. The Use of the Slip Circle in the Stability Analysis of Slopes. Geotechnique, Vol. 5, No. 1, March 1955, pp. 7-17.
13. E.H. Vanmarcke. On the Scale of Fluctuation of Random Functions. Department of Civil Engineering, Massachusetts Institute of Technology, Cambridge, Res. Rept. R79-17, April 1979.
14. W.A. Bailey and J.T. Christian. ICES LEASE-1: A Problem-Oriented Language for Slope Stability Analysis--User's Manual. Department of Civil Engineering, Massachusetts Institute of Technology, Cambridge, Soil Mechanics Publ. 235, April 1969.
15. H.B. Dwight. Probability Integrals. In Tables of Integrals and Other Mathematical Data, Macmillan, New York, 1961, p. 136.
16. P. Lumb. The Variability of Natural Soils. Canadian Geotechnical Journal, Vol. 3, No. 2, 1966, pp. 74-97.

*Publication of this paper sponsored by Committee on Mechanics of Earth Masses and Layered Systems.*

# Reliability of Soil Slopes

L. ALFARO AND M.E. HARR

**Results of a study of the safety of soil slopes are reported in which the measure of safety used is "reliability" (or the "probability of failure"), an a priori quantitative estimate of the likelihood of the safety (or failure) of a slope. A closed-form solution to determine slope reliability is proposed in which a material with two resistance parameters (c and tan $\phi$) is accommodated. Input to the model consists of a bivariate distribution of c and tan $\phi$ for the slope material and a line called the "critical boundary", which is independent of the operative strength parameters. This line is the locus of points in the c tan $\phi$ plane for which the slope in question is in a state of limiting equilibrium (factor of safety equal to unity). Beta distributions are assumed to model the variability of c and tan $\phi$. The critical boundary is determined from two-dimensional and three-dimensional slope-stability analyses. For the former, the ordinary method of slices is adopted because of its simplicity (it requires no iterations) and because it is the only method that does not make the unrealistic assumption that the factor of safety takes the same value along the entire slip surface, thus permitting the analysis to yield some information regarding the failure process. For the three-dimensional analysis, Hovland's method is used. In concept, it is the three-dimensional equivalent of the ordinary method of slices. Output from the model is the probability of failure of the slope, which is information dependent and therefore can vary as new information is obtained. These probabilities can then be used to place the problem in the framework of decision theory.**

Current procedures for evaluating the safety of slopes consist in determining a factor of safety (1-4) that is compared with allowable values found to be satisfactory on the basis of previous experience. The factor of safety suffers from the following:

1. Elements of uncertainty in analyses are not quantified when the factor of safety is used.
2. The scale of the factor of safety (F) is not known. For example, a structure with a factor of safety of 3.0 is not necessarily twice as safe as another with a factor of safety of 1.5.
3. Allowable values to be selected for the factor of safety are the result of experience. In dealing with new or different problems for which there is no previous experience, there is no allowable factor of safety.

To overcome these difficulties and permit the engineer to predict the performance of his or her designs, the concept of "reliability" or "probability of failure" is recommended (5-7).

Probability itself is a subjective interpretation. According to the definition of Tribus (8), "A probability assignment is a numerical encoding of a state of knowledge." A probability is understood to be an information-dependent quantity that may not be intrinsically related to the physical world. That is, the estimate of the reliability of a structure may change as new information regarding it is obtained, although the structure itself would remain unaltered.

This paper introduces a procedure to determine reliability that involves no approximations (from a probabilistic point of view) and can accommodate a material with the two customary operative strength parameters--i.e., "c" and "tan $\phi$" = "t" (tan $\phi$ is designated t for simplicity).